

2010

Experimental Study of Frost Accumulation on Fan-Supplied Tube-Fin Evaporators

Diogo Da Silva

Federal University of Santa Catarina

Christian Hermes

Federal University of Parana

Claudio Melo

Federal University of Santa Catarina

Follow this and additional works at: <http://docs.lib.purdue.edu/iracc>

Silva, Diogo Da; Hermes, Christian; and Melo, Claudio, "Experimental Study of Frost Accumulation on Fan-Supplied Tube-Fin Evaporators" (2010). *International Refrigeration and Air Conditioning Conference*. Paper 1013.
<http://docs.lib.purdue.edu/iracc/1013>

This document has been made available through Purdue e-Pubs, a service of the Purdue University Libraries. Please contact epubs@purdue.edu for additional information.

Complete proceedings may be acquired in print and on CD-ROM directly from the Ray W. Herrick Laboratories at <https://engineering.purdue.edu/Herrick/Events/orderlit.html>

Experimental Study of Frost Accumulation on Fan-Supplied Tube-Fin Evaporators

Diogo L. da SILVA^{1*}, Christian J. L. HERMES², Cláudio MELO¹

¹ POLO Research Laboratories for Emerging Technologies in Cooling and Thermophysics,
Department of Mechanical Engineering, Federal University of Santa Catarina
88040-970, Florianópolis, SC, BRAZIL

² Department of Mechanical Engineering, Federal University of Paraná,
P.O. Box 19011, 81531-990, Curitiba, PR, BRAZIL

* Corresponding Author, Phone: ++55 48 3234 5691, e-mail: diogo@polo.ufsc.br

ABSTRACT

Compact tube-fin evaporators have been extensively used in refrigeration cassettes for light commercial applications. Such refrigeration systems are space constrained and, therefore, the heat exchangers (condenser and evaporator) must have a large area-to-volume ratio. In addition, such applications require a subfreezing evaporating temperature that induces the growth of a frost layer on the finned surface, which may block the evaporator if a proper defrost strategy is not used. Before completely blocking the evaporator, the frost layer depletes the heat exchanger performance by adding an extra thermal resistance and also by reducing the fan-supplied air flow rate. Understanding the way the frost forms on these compact heat exchangers and also the way the fan is affected by frost clogging is mandatory for the design of robust refrigeration systems and also to devise more efficient defrost strategies. In this study an experimental investigation on the frost accretion of tube-fin evaporators considering the fan characteristics is carried out. To this end, a specially designed, constructed and calibrated closed-loop wind-tunnel facility was used. Nine experimental tests were carried out with two different evaporator coils under different conditions. It was found that the fan characteristics play an important role in the evaporator thermal performance, indicating that for frosting conditions the fan and evaporator designs cannot be dissociated from one other.

1. INTRODUCTION

The efficient use of energy resources is a fundamental issue, not only due to its inherent environmental appeal but also to the steadily increasing energy costs, encouraging changes in the way energy is generated, distributed and consumed. Since the refrigeration sector is responsible for a large amount of the energy consumed worldwide, most governments are launching energy consumption policies to stimulate the development of highly efficient refrigeration systems. However, the development of such a class of refrigeration systems relies not only on the component designs (e.g., high efficiency compressors, anti-fouling condensers and no-frost evaporators) but also on a proper matching between them.

The medium back pressure (MBP) light commercial refrigeration appliances usually run with evaporating temperatures close to -10°C , a temperature that favors the formation of a frost layer on the evaporator coil. The frost accumulated on the evaporator decreases dramatically the heat exchanger performance due to the combined effect of the low thermal conductivity of the frost layer and the reduced fan-supplied air flow rate. This double-effect was firstly investigated by Stoecker (1957), who carried out an experimental study on the effect of frost formation on the overall heat transfer coefficient and air-side pressure drop of industrial evaporators.

However, in spite of its importance, evaporator frosting research remained latent for many years until the 1990s, when Rite and Crawford (1991) conducted an experimental study on domestic finned-tube heat exchangers under frosting conditions and observed an increase in the air-side pressure drop and overall heat transfer coefficient, the latter being explained by an increase in the heat transfer surface area and a decrease in the thermal contact resistance

between the fins and tubes. Later, Bejan *et al.* (1994) also studied the performance of refrigeration systems operating under frosting conditions. The authors assumed a constant frost formation rate and identified an optimal on/off control strategy that minimizes the energy consumption of the whole system taking the electrical power of the defrost heaters into account. However, the above-mentioned studies did not account for the non-linear effect induced by the combination of the frosted evaporator and the fan-supplied air flow rate.

In a first attempt to fill this gap, Xia *et al.* (2006) studied the frosting, defrosting and re-frosting processes taking place on louvered-fin flat-tube heat exchangers and observed that the overall heat transfer coefficient decreases due to the reduction in the air flow rate and also to the bridging of louver gaps. The authors concluded that the initial air pressure drop increases after each defrosting cycle due to the retention of condensed water droplets that subsequently re-frost. Although this study revealed important information on some of the factors affecting the frost formation phenomenon, a specific investigation with regard to fan-supplied tube-fin evaporators with cooling capacities typical of light commercial refrigerators (~ 500 W) has not, as yet, been performed. Thus, this topic is the main focus of this paper.

2. EXPERIMENTAL WORK

2.1 Experimental facility

The experimental apparatus is comprised of a rectangular cross-section closed loop wind-tunnel test facility and a secondary refrigeration system. The former is used to control the air temperature, humidity and flow rate at the evaporator inlet, and the latter sets the evaporator surface temperature. Figure 1 shows a schematic representation of the test rig, which is divided into the lower part, where the air is conditioned, and the upper part, where the tests are carried out. In the lower part the air firstly flows through a 6.35 cm nozzle (1) used to measure the air flow rate according to the ASHRAE 51 (1999) standard, with a maximum uncertainty of ± 0.003 m³/s. The air is then cooled down by a coil (2), re-heated by an electric heater (3) and re-humidified by a water tray (4). All these processes are PID-controlled in order to guarantee the desired psychrometric conditions at the inlet of the test section. The air flow rate is controlled by a computer-controlled variable-speed fan (5).

In the upper part of the test rig, air temperature, relative humidity and pressure measurements are made upstream and downstream of the evaporator (EVAP). The air temperature is measured by two grids of nine T-type thermocouples (TT) each, with a maximum uncertainty of $\pm 0.2^\circ\text{C}$. The relative humidity is measured by two capacitive humidity transducers (HT) that provide a maximum uncertainty of $\pm 1.5\%$ (RH). The air side pressure drop through the evaporator coil is measured by a differential pressure transducer (PT) with a maximum uncertainty of ± 2.5 Pa. The frost formation rate and the heat transfer rate are indirectly measured by mass and energy balances, with uncertainties of ± 0.1 kg/h and ± 80 W, respectively.

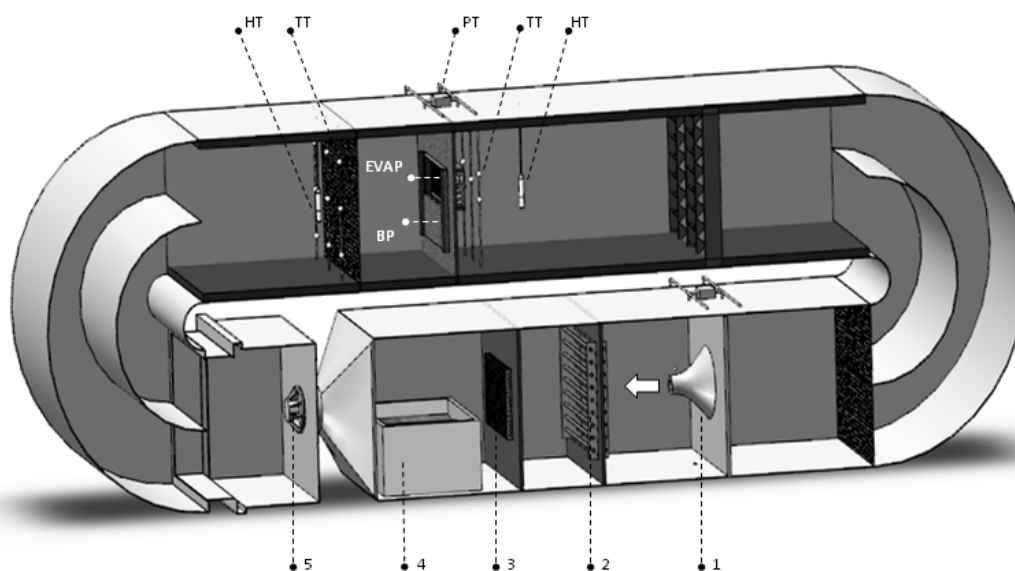


Figure 1. Schematic representation of the test rig

The evaporator (EVAP) is fastened onto a wooden structure where a damper directs the air flow either to its front surface or to a by-pass (BP) opening located below the coil. This device guarantees that the frost accumulation process only starts when the testing conditions have been properly reached. A chilled ethylene-glycol-water solution flows through the coil in such a way as to establish the evaporator surface temperature, with a maximum temperature difference between its inlet and exit ports of 3.5°C.

The evaporator is a finned circular tube cross-flow heat exchanger, as shown in Fig. 2. The wavy-type fins are made of an aluminum alloy with a thickness of 0.2 mm. The copper tubes have an outer diameter of 10 mm and a wall thickness of 1 mm. The evaporator is 320 mm wide, 152 mm high and 45 mm deep. The tubes are arranged in two rows, with six tubes per row. The longitudinal and transversal spacing between two adjacent tubes are 22 mm and 25 mm, respectively.

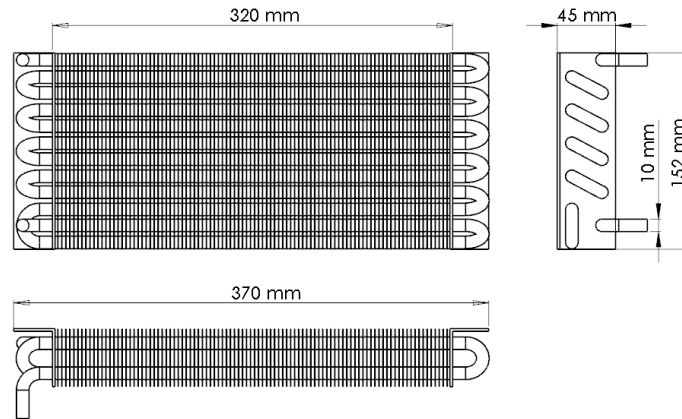


Figure 2. Schematic representation of the evaporator under testing

The air flow rate is controlled by a computer-driven variable-speed centrifugal fan that emulates the performance characteristics of fans typically found in light commercial refrigeration systems. The fan emulation procedure follows an iterative process, which converges when the difference between the actual and required air flow rates is less than 2%. Figure 3 shows the pressure versus air flow rate performance characteristics of an axial fan, emulated by the test rig centrifugal fan. Therefore, frost accumulation tests can be carried out with a constant or variable air flow rate.

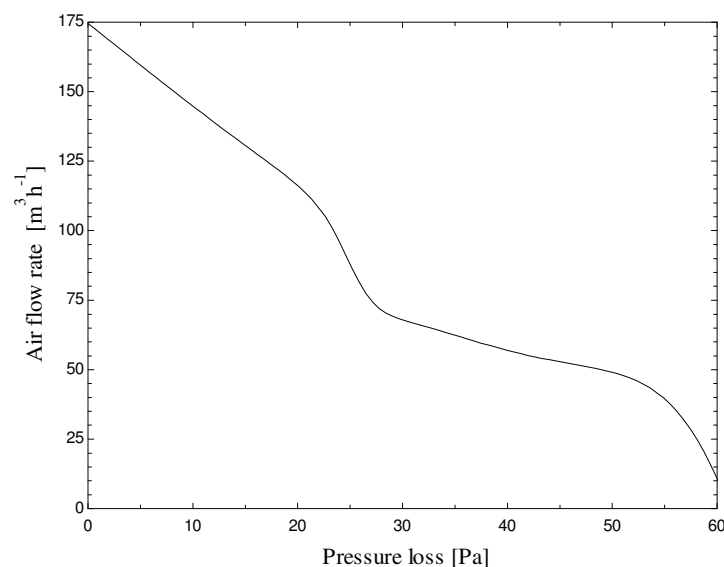


Figure 3. Performance characteristics of an emulated axial fan

2.2 Data reduction

The frost accumulation rate, the total heat transfer rate and the air pressure drop were derived from mass, energy and momentum balances over the evaporator, as follows:

$$m_f = m(\omega_1 - \omega_2) \quad (1)$$

$$M_f = \int m_f dt \quad (2)$$

$$\Delta p = p_1 - p_2 \quad (3)$$

$$q_{sen} = mc_{p,a}(T_1 - T_2) + \beta(T_{sur} - T_1) \quad (4)$$

$$q_{lat} = m_f L \quad (5)$$

$$q = q_{sen} + q_{lat} \quad (6)$$

where m_f represents the frost accumulation rate [kg s^{-1}], m is the air flow rate [kg s^{-1}], ω is the humidity ratio [kg_s/kg_a], M_f is the accumulated frost mass [kg], t is the time [s], p is the air pressure [Pa], q_{sen} is the sensible heat transfer rate [W], $c_{p,a}$ is the air specific heat at constant pressure [$\text{J kg}^{-1} \text{K}^{-1}$], T is the temperature [K], β is an empirical correction coefficient [W K^{-1}], q_{lat} is the latent heat transfer rate [W], L is the latent heat of desublimation [$\text{J kg}^{-1} \text{K}^{-1}$] and q is the cooling capacity [W]. It is worth noting that as the heat transfer process is dependent on both the temperature and humidity ratio differences, the overall heat transfer coefficient was calculated based on the air enthalpies as suggested by Threlkeld *et al.* (1998),

$$U_h = \frac{q}{A_{wf} \Delta h_m} \quad (7)$$

$$\Delta h_m = \frac{(h_1 - h_{s,r2}) - (h_2 - h_{s,r1})}{\ln \left(\frac{h_1 - h_{s,r2}}{h_2 - h_{s,r1}} \right)} \quad (8)$$

where U_h is the overall heat transfer coefficient [$\text{W m}^{-2} \text{kg}_a \text{J}^{-1}$], A_{wf} is the evaporator surface area [m^2], Δh_m is the log-mean air enthalpy difference [J kg_a^{-1}], h_1 and h_2 are the moist air enthalpies [J kg_a^{-1}] at the evaporator inlet and outlet, respectively, and $h_{s,r1}$ and $h_{s,r2}$ are the saturated moist air enthalpies [J kg_a^{-1}] at the refrigerant entering and leaving temperatures, respectively.

2.3 Test plan

The tests were intended to investigate the effect of the fin density, air temperature and humidity, evaporator surface temperature and air flow rate on the evaporator air pressure drop, cooling capacity and accumulated frost mass. Supercooling levels (i.e., the temperature difference between the evaporator surface and the dew-point of the entering air flow, see Hermes *et al.*, 2009) of 3.5, 5.0, 10.0 and 14.5°C were used in combination with different air flow rates and evaporator geometries (i.e., different fin densities). Table 1 summarizes the test conditions, which cover the ranges typical of light commercial refrigeration applications. The experimental runs were conducted until the evaporator air flow rate or the total test time reached 60 m^3/h and 120 min, respectively.

Table 1. Summary of the experimental conditions

Test No.	Fin density [fins/cm]	Supercooling [°C]	T_1 [°C]	ϕ [%]	T_{evap} [°C]	Air flow rate [m^3/h]
1	3.2	10.0	2.5	85	-10	150
2	3.2	14.5	7.0	85	-10	Fan curve
3	3.2	10.0	2.5	85	-10	Fan curve
4	3.2	5.0	2.5	85	-5	Fan curve
5	3.2	3.5	2.5	74	-5	Fan curve
6	4.7	14.5	7.0	85	-10	Fan curve
7	4.7	10.0	2.5	85	-10	Fan curve
8	4.7	5.0	2.5	85	-5	Fan curve
9	4.7	3.5	2.5	74	-5	Fan curve

3. RESULTS AND DISCUSSION

Figure 4 shows the time evolution of the frost accretion on the evaporator surface. It can be seen that an increase in the fin density or in the level of supercooling increases the frost accumulation rate. Also, the frost accumulation rate decreases over time, especially for the tests carried out with supercooling values of 10.0 and 14.5°C, since both the frost surface temperature and the fan-supplied air flow rate also decrease over time. Figure 5 shows photographs taken at the beginning and end of a 35-min experiment carried out with an air flow rate of 150 m³/h, air temperature of 10°C, relative humidity of 50% and inlet refrigerant temperature of -10°C. A significant reduction in the evaporator free flow area can be observed, which has a considerable effect on the heat exchanger thermal-hydraulic performance. It should be noted that all analyses were carried out using the supercooling value as an independent variable since this parameter brings together all the information associated with the independent variables (p , T_a , ϕ and T_{evap}) of the process.

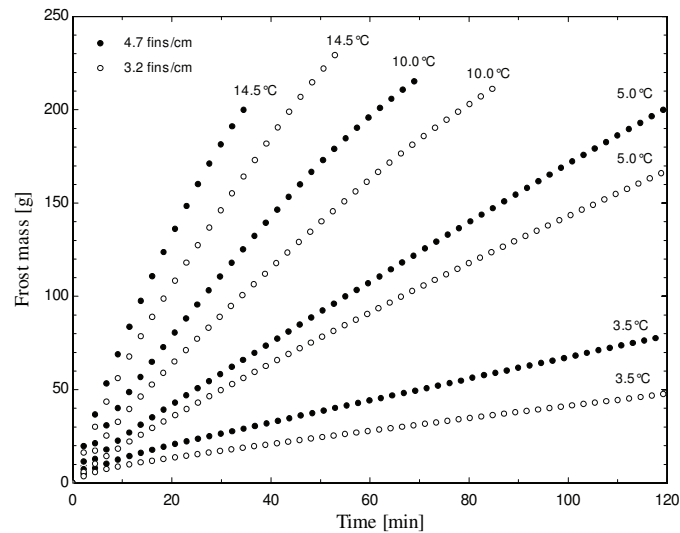


Figure 4. Accumulated frost mass for different fin densities and supercooling values

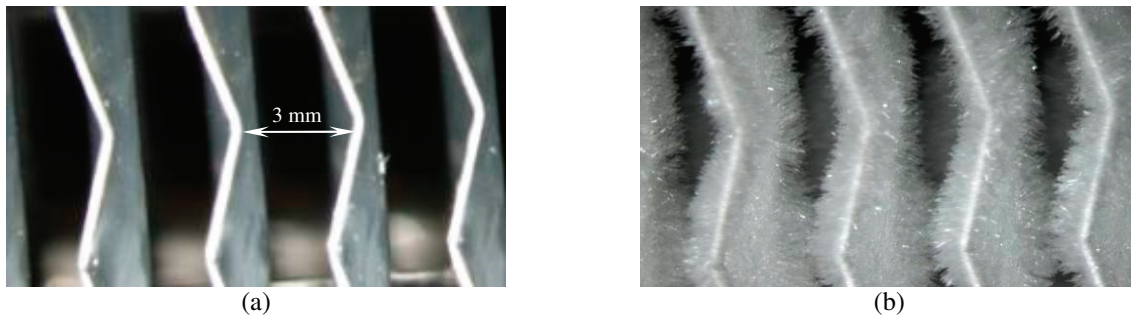


Figure 5. Visualization of the fin surface before (a) and after (b) the frost accumulation process

Figure 6 shows the influence of the accumulated frost mass on the air-side pressure drop, where it is shown that the supercooling and the fin density both increase the air pressure drop. It can also be observed that at a low level of supercooling (i.e., 3.5°C) the pressure drop remains almost constant since the accumulated frost mass under these conditions is small. Figure 7 illustrates the effect of the accumulated frost mass and thus of the air pressure drop on the fan-supplied air flow rate. It is worth noting that the air flow rate is dramatically reduced, especially at supercooling values of 10.0 and 14.5°C, where reductions of 50% can be observed within 30 to 70 min, depending on the fin density and level of supercooling.

Figure 8 shows the effect of the accumulated frost mass on the evaporator cooling capacity. As expected the evaporator performance increases with the level of supercooling and fin density. It can also be noted that after 30 min the cooling capacity of the 4.7-fins/cm evaporator, with a supercooling value of 14.5°C, drops by 40%, reaching

a heat transfer rate similar to that observed with the 3.2-fins/cm evaporator at the same supercooling level. From this time onward the 4.7-fins/cm evaporator cooling capacity is surpassed by that of the 3.2-fins/cm evaporator. Figure 8 also shows a comparison between the experiments carried out with constant and variable air flow rates (Tests 1 and 3 in Table 1). It should be noted that with a constant air flow rate the evaporator cooling capacity drops by only 15% after a test period of 80 min, a reduction considerably smaller than that obtained with a variable air flow rate (40%). These figures reveal that the reduction in the air flow rate has a greater impact on the evaporator performance than the extra thermal resistance of the frost layer. The overall heat transfer coefficient as a function of time is plotted in Fig. 9, where it is shown that the evaporator U_h value remains almost constant under low supercooling conditions, in contrast to the behavior observed under high supercooling conditions.

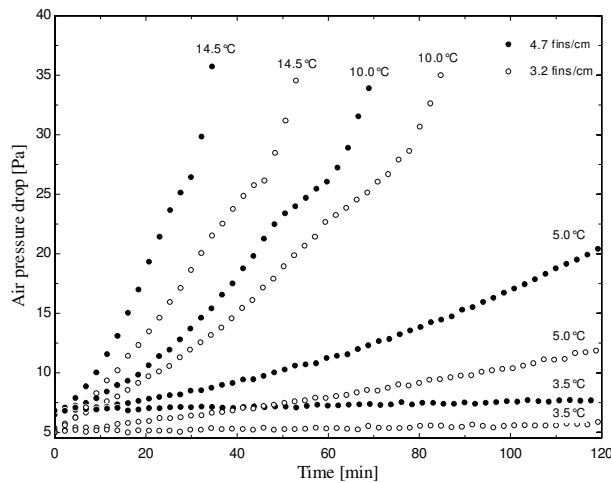


Figure 6. Evaporator air-side pressure drop for different fin densities and supercooling values

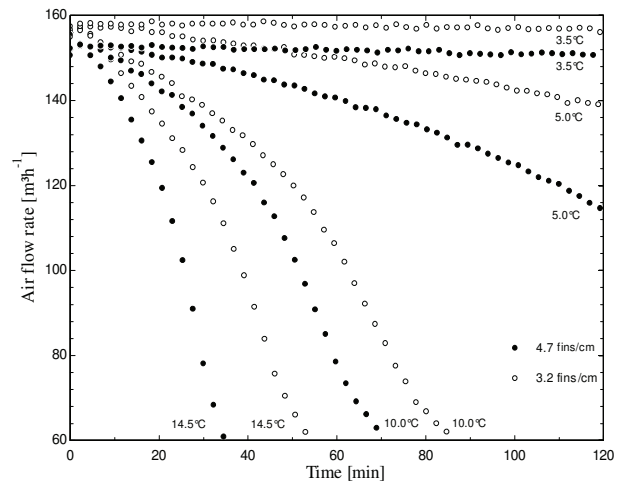


Figure 7. Fan-supplied air flow rate for different fin densities and supercooling values

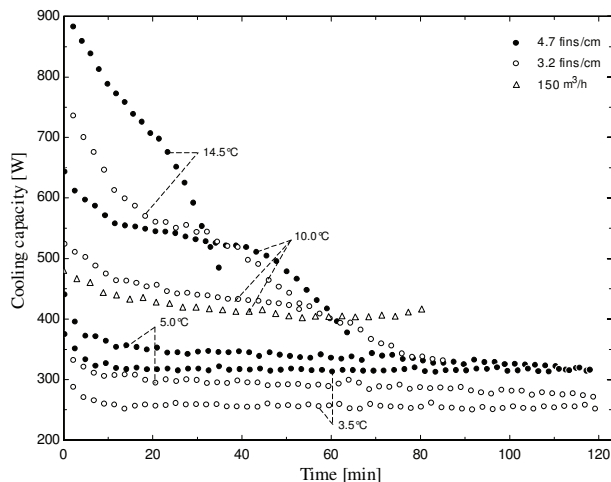


Figure 8. Cooling capacity for different fin densities and supercooling values

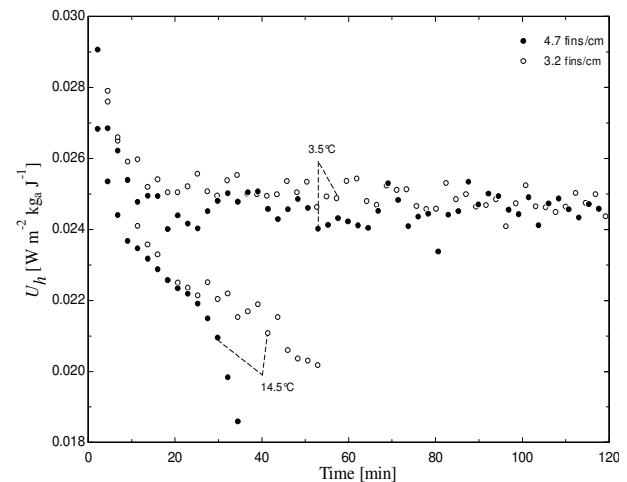


Figure 9. Overall heat transfer coefficient for different fin densities and supercooling values

4. CONCLUDING REMARKS

A purpose-built experimental facility was designed and constructed specifically to investigate the effect of frost accumulation on the thermo-hydraulic performance of tube-fin evaporators. The test facility is comprised of a closed-loop wind-tunnel which controls and measures the brine and air flow properties and emulates the product fan characteristics. The tests were carried out with two tube-fin heat exchangers operating at different evaporating and inlet air temperatures and relative humidity values. It was observed that the frost accumulation rate increases with the air flow rate, supercooling value and fin density. A strong relation between the accumulated frost mass, air-side pressure drop and cooling capacity was also observed. Furthermore, it was shown that the effect of the reduction of

the air flow rate on the evaporator cooling capacity surpasses that of the extra thermal insulation of the frost layer. The results also indicate that for frosting conditions the fan and evaporator designs can not be dissociated from one other.

REFERENCES

- ASHRAE Standard 51, 1999, Laboratory methods of testing fans for aerodynamic performance rating, *American Society of Heating, Refrigeration and Air Conditioning Engineers*, Atlanta, GA.
- Bejan, A., Vargas, J. V. C., Lim, J. S., 1994, When to defrost a refrigerator, and when to remove the scale from the heat exchanger of a power plant, *International Journal of Heat and Mass Transfer*, Vol. 37(3), pp. 523-532.
- Hermes, C. J. L., Piucco, R. O., Barbosa, Jr, J. R., Melo, C., 2009, A study of frost growth and densification on flat surfaces, *Experimental Thermal and Fluid Science*, Vol. 33, pp. 371-379.
- Rite, R. W., Crawford, R. R., 1991, The effect of frost accumulation on the performance of domestic refrigerator-freezer finned-tube evaporator coils, *ASHRAE Transactions*, Vol. 97(2), pp. 428-437.
- Stoecker, W. F., 1957, How frost formation on coils affects refrigeration systems, *Refrigerating Engineering*, Vol. 65, no. 2.
- Threlkeld, J. L., Kuehn, T. H., Ramsey, J. W., 1998, *Thermal Environmental Engineering*, 3rd ed., Prentice-Hall.
- Xia, Y., Zhong Y., Hrnjak, P. S., Jacobi, A. M., 2006, Frost, defrost, and re-frost and its impact on the air-side thermal-hydraulic performance of louvered-fin, flat-tube heat exchangers, *International Journal of Refrigeration*, Vol. 29, pp. 1066-1079.

ACKNOWLEDGEMENTS

This study was carried out at the POLO facilities under National Grant No. 573581/2008-8 (National Institute of Science and Technology in Refrigeration and Thermophysics) funded by the CNPq Agency. Financial support from Embraco S.A. is also duly acknowledged. The authors also thank Mr. Elias G. Colombo and Miss Giulia Baretta, undergraduate students, for their valuable support with the experiments.

NOMENCLATURE

Roman

A_{wf}	evaporator free flow area [m ²]
$c_{p,a}$	specific heat at constant pressure [J kg ⁻¹ K ⁻¹]
h	air enthalpy [J/kg]
L	latent heat of desublimation [J kg ⁻¹ K ⁻¹]
m	air mass flow rate [kg s ⁻¹]
m_f	frost accumulation rate [kg s ⁻¹],
M_f	accumulated mass frost mass [kg]
p	air pressure [Pa]
q	cooling capacity [W]
t	time [s]
T	temperature [K]
U_h	heat transfer coefficient [W m ⁻² kg _a J ⁻¹]

Greek

β	empirical correction coefficient [W K ⁻¹]
---------	---

ϕ	relative humidity [%]
ω	humidity ratio [kg _s kg ⁻¹ _a]

Subscripts

a	dry air
$evap$	evaporator
f	frost
lat	latent
m	mean
s	steam
s,r	saturated at refrigerant temperature
sen	sensible
sur	surroundings
1	inlet
2	outlet